



Tailoring Ferrimagnetic Transition Temperatures, Coercivity Fields, and Saturation Magnetization by Modulating Mn Concentration in $(\text{CoCrFeNi})_{1-x}\text{Mn}_x$ High-Entropy Alloys

Chi-Hung Lee^{1*}, Hsu-Hsuan Chin², Kun-Yuan Zeng², Yao-Jen Chang^{3,4}, An-Chou Yeh^{3,4}, Jien-Wei Yeh^{3,4}, Su-Jien Lin^{3,4}, Chun-Chieh Wang^{1,4*}, Uwe Glatzel⁵ and E-Wen Huang^{2,4*}

¹National Synchrotron Radiation Research Center, Hsinchu, Taiwan, ²Department of Materials Science and Engineering, National Yang Ming Chiao Tung University, Hsinchu, Taiwan, ³Department of Materials Science and Engineering, National Tsing Hua University, Hsinchu, Taiwan, ⁴High Entropy Materials Center, National Tsing Hua University, Hsinchu, Taiwan, ⁵Metals and Alloys, University of Bayreuth, Bayreuth, Germany

OPEN ACCESS

Edited by:

Dongchan Jang,
Korea Advanced Institute of Science
and Technology, South Korea

Reviewed by:

Rajesh K. Mishra,
IFTM University, India
Fuyang Tian,
University of Science and Technology
Beijing, China

*Correspondence:

Chi-Hung Lee
lee.ch@nsrc.org.tw
Chun-Chieh Wang
wang.jay@nsrc.org.tw
E-Wen Huang
ewhuang@g2.nctu.edu.tw

Specialty section:

This article was submitted to
Mechanics of Materials,
a section of the journal
Frontiers in Materials

Received: 29 November 2021

Accepted: 07 January 2022

Published: 28 January 2022

Citation:

Lee C-H, Chin H-H, Zeng K-Y,
Chang Y-J, Yeh A-C, Yeh J-W, Lin S-J,
Wang C-C, Glatzel U and Huang E-W
(2022) Tailoring Ferrimagnetic
Transition Temperatures, Coercivity
Fields, and Saturation Magnetization
by Modulating Mn Concentration in
 $(\text{CoCrFeNi})_{1-x}\text{Mn}_x$ High-
Entropy Alloys.
Front. Mater. 9:824285.
doi: 10.3389/fmats.2022.824285

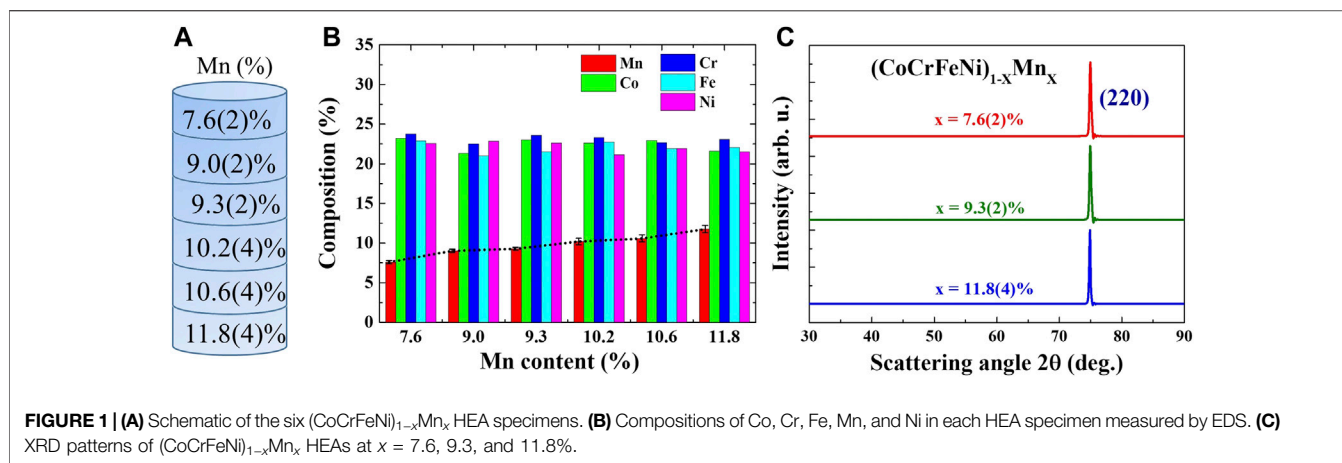
Cr and Mn play intriguing roles in determining the magnetic properties of CoFeNi-based high-entropy alloys (HEA). In this study, we tune the stoichiometric Mn composition to systematically explore the magnetic properties of $(\text{CoCrFeNi})_{1-x}\text{Mn}_x$ HEAs. We observe a change from ferro-to ferrimagnetism due to the incorporation of Mn atoms into the CoCrFeNi HEA. In addition, we measure an 81% reduction in magnetization with the incorporation of 7.6 (2)% Mn atoms. Such a significant reduction in magnetization cannot be solely explained by the effect of the inversed moments on the Mn atoms. Hence, we propose a mechanism whereby the Mn atoms flip the moments of neighboring atoms, which results in the magnetization reduction observed in the CoFeNi-based HEAs.

Keywords: ferrimagnetism, high-entropy alloy (HEA), single crystal, magnetization, ferromagnetism

INTRODUCTION

High-entropy alloys (HEA) are promising for their potential and their possible applications (George et al., 2019). Among the studies on HEAs (Yeh et al., 2004; Otto et al., 2013; Gludovatz et al., 2014; Cong et al., 2016; Ye et al., 2016), research into their magnetic properties is challenging because the geometry of HEAs, whether in bulk, powder, or thin-film forms, can change their magnetic performance, even when the stoichiometries of the HEA composition are identical (Huang et al., 2020). Regardless, owing to their good mechanical performance (Otto et al., 2013; Gludovatz et al., 2014), magnetic applications of HEAs are hotly anticipated (Koželj et al., 2019; Huang et al., 2020; Chaudhary et al., 2021; Na et al., 2021). Meanwhile, the exchange couplings between the many elements of HEAs bring greater complexity for research and development. For example, FeCoNiPdCu HEAs exhibit excellent magnetic softness (Koželj et al., 2019). HEAs can also have tunable hard magnetism, which can be realized by making minor changes to the stoichiometry of the elements (Na et al., 2021).

In investigations focused on the effects of various elements on magnetic properties, the roles played by Cr and Mn in CoFeNi-based HEAs are particularly intriguing. The magnetic moments of Co, Fe, and Ni are known to make them ferromagnetic, and those of Cr are known to make them antiferromagnetic. On the other hand, Mn atoms exhibit multipole magnetic states (Song et al.,



2017). However, when either Cr or Mn atoms are incorporated into CoFeNi HEAs, such as CoCrFeNi (Kao et al., 2011; Lucas et al., 2013; Chaudhary et al., 2020) and CoFeMnNi (Hariharan et al., 2020), the HEAs unexpectedly remain ferromagnetic. Some studies show that incorporating both Cr and Mn into HEAs, such as in CoCrFeMnNi, leads to antiferromagnetism (Schneeweiss et al., 2017; Zuo et al., 2017) while, in contrast, other studies report ferromagnetism in CoCrFeMnNi HEAs (Acet, 2019). The interactions between neighboring Mn, Cr, and other elements in HEAs and the associated mechanisms have thus not yet been conclusively defined.

In this work, we systematically explore the magnetic properties of $(\text{CoCrFeNi})_{1-x}\text{Mn}_x$ HEAs by tuning the stoichiometric Mn composition. We found that Mn-free CoCrFeNi is ferromagnetic, whereas Mn-incorporated $(\text{CoCrFeNi})_{1-x}\text{Mn}_x$ HEAs is ferrimagnetic. Interestingly, the marked reduction of magnetization caused by a small amount of Mn atoms suggests that some of the Co, Cr, Fe, and Ni magnetic moments may be flipped by exchange interactions with the Mn atoms.

MATERIALS AND METHODS

We cast single crystals of $(\text{CoCrFeNi})_{1-x}\text{Mn}_x$ HEAs in a proprietary Bridgman furnace. The master alloy was formed from high-purity elements (>99.9%) in an arc furnace under a 500 mbar Ar atmosphere. We conducted subsequent single-crystal casting with a temperature gradient of 6 K/mm and a withdrawal rate of 3 mm/min. The vapor pressure of the Mn was relatively lower than that of the other elements. The Mn evaporated significantly during the growing of the single crystal, resulting in a gradient in the Mn composition, as shown in **Figure 1A**. We cut the single crystal perpendicular to the Mn gradient into six pieces *via* wire electrical discharge machining.

We used X-ray diffraction (XRD), scanning electron microscopy (SEM), and energy-dispersive X-ray spectroscopy (EDS) to characterize the single crystals. We performed the XRD measurements on a Bruker D8 Discover diffractometer,

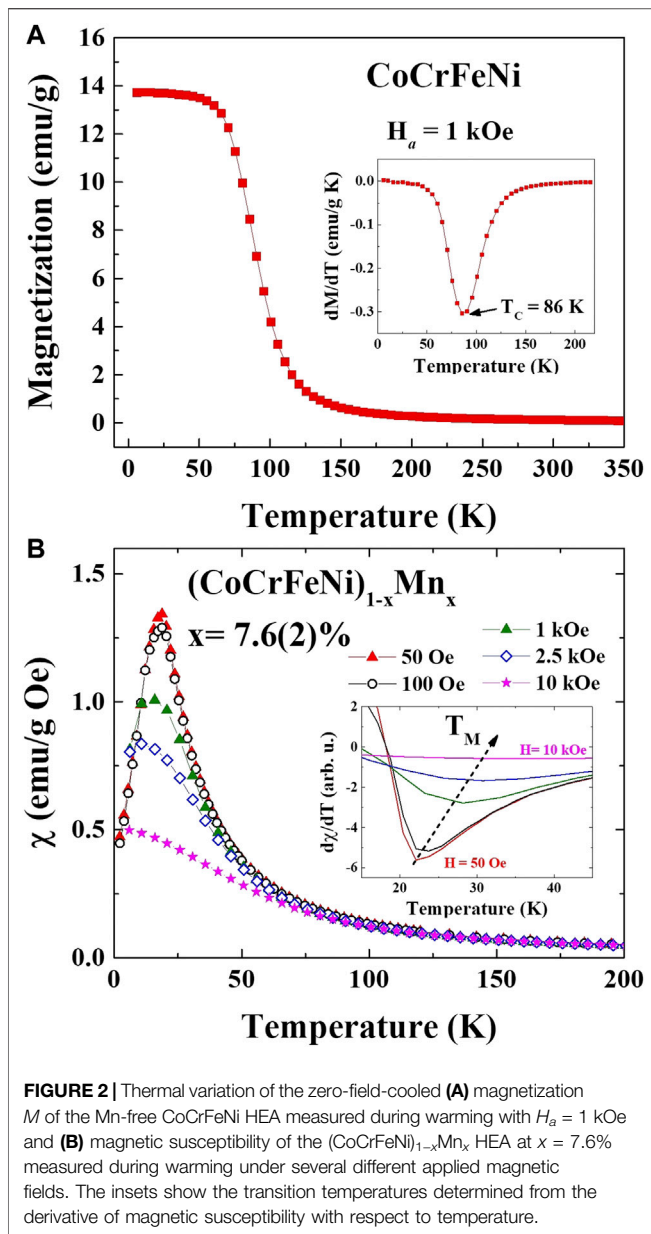
employing the standard setup for reflection geometry. We observed the EDS spectra with an Oxford MAX150 detector attached to a JEOL JSM-7800F PRIME scanning electron microscope employing a standard setup to analyze three portions each of size $75 \times 60 \mu\text{m}$ for every sample. We measured the magnetization using an MPMS 3 SQUID, manufactured by Quantum Design, Inc., employing the standard setup.

Figure 1B shows the results of the EDS analysis for each HEA. We performed the EDS measurements on both sides of all the investigated specimens, giving average values for each element in the composition. There was no obvious variation in the Co, Cr, Fe, and Ni contents in each HEA sample. However, there was a significant gradient from 7.6 (2)% to 11.8 (4)% in Mn content. The samples with different Mn contents are hereafter designated as $(\text{CoCrFeNi})_{1-x}\text{Mn}_x$ HEAs with $x = 7.6\text{--}11.8\%$.

From the XRD patterns, the reflections can be indexed as (220) based on the face-centered cubic (FCC) structure, as shown in **Figure 1C**. No reflection other than (220) was detected, indicating the sampled HEA sections were from a single-crystalline-structure region. There were no identifiable traces of impurity phases in the XRD patterns. The lattice constants increased from 3.583 to 3.587 Å as the Mn content increased from $x = 7.6\text{--}11.8\%$. The atomic radius of the Mn atom is relatively large compared to that of Co, Cr, Fe, and Ni, and results in an increase in the lattice constants.

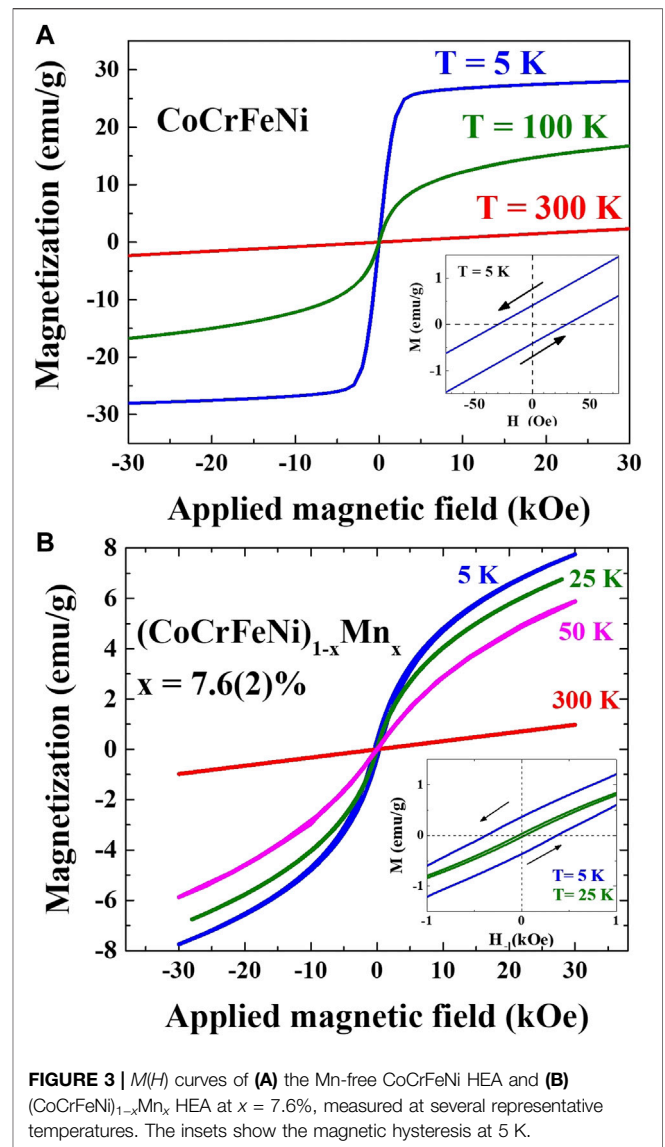
RESULTS AND DISCUSSION

Figure 2A displays the temperature dependency of the magnetization, $M(T)$, of the Mn-free CoCrFeNi HEA in the zero-field-cooled process. A transition at 86 K can be clearly observed in dM/dT (inset in **Figure 2A**). The $M(T)$ curve follows the Curie-Weiss law $M = C/(T - \theta)$, as shown in **Supplementary Figure S1**, where C is the Curie constant and θ is the Weiss constant. The negative intercept of the $1/M$ trace with the temperature axis indicates a ferromagnetic behavior (Kittel et al., 1996). By calculating the Curie constant as $C = N\mu_{\text{eff}}^2/3k_B$, an effective magnetic moment of $3.16 \mu_B$ can be obtained.



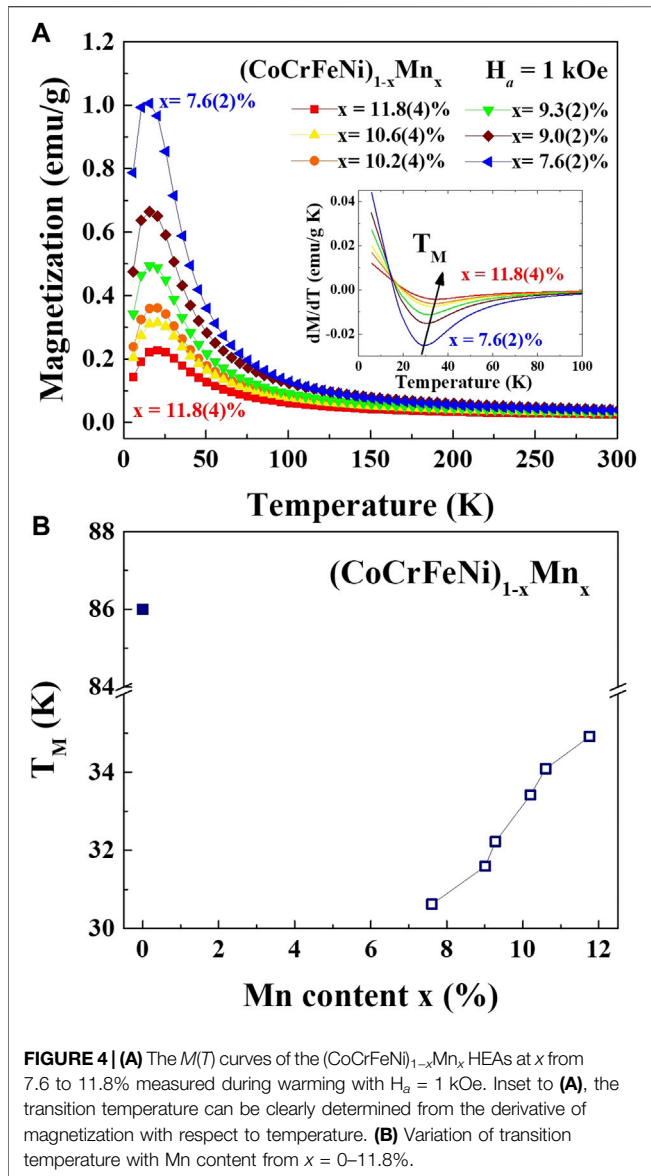
The effective moment is less than the calculated average spin-only value of $4.38 \mu_B$ found among Co, Cr, Fe, and Ni based on the equimolar composition ($3.87 \mu_B/\text{Co}$, $5.92 \mu_B/\text{Cr}$, $4.90 \mu_B/\text{Fe}$, and $2.83 \mu_B/\text{Ni}$). The positive Weiss constant $\theta = 122$ K indicates a ferromagnetic interaction between the magnetic elements.

Interestingly, the incorporation of the Mn atoms into the CoCrFeNi HEA changes its magnetic behavior significantly. The temperature dependency of the dc magnetic susceptibility, $\chi(T)$, of the (CoCrFeNi)_{1-x}Mn_x HEA at $x = 7.6\%$ is shown in **Figure 2B**. Here, the dc magnetic susceptibility χ is the magnetization divided by the applied magnetic field. A peak at ~ 20 K was clearly revealed in the low magnetic fields. However, it was suppressed by the applied magnetic field, thus showing the alignment of the antiparallel spins. The inverse $M(T)$ curves follow the Curie–Weiss law (**Supplementary Figure S1**). The



positive intercept of the $1/M$ trace with the temperature axis also suggests the antiparallel alignment of the magnetic moments (Kittel et al., 1996). However, the transition temperatures, as shown in the inset in **Figure 2B**, increase with the applied magnetic fields, suggesting ferromagnetic-like behavior. Normal ferrimagnetism exhibits both ferromagnetic and antiferromagnetic properties. Although antiparallel moments exist, they do not exactly cancel out. The net moments produce ferromagnetic behaviors. Combining these two arguments, namely 1) the existence of the antiparallel moments and 2) the ferromagnetic-like transition temperatures, we propose the occurrence of ferrimagnetism in (CoCrFeNi)_{1-x}Mn_x HEA.

The field dependency of the isothermal magnetization, $M(H)$, taken at several representative temperatures, of the Mn-free CoCrFeNi HEA is shown in **Figure 3A**, where H is the applied magnetic field. The magnetization increases rapidly at small H values and saturates at ~ 5 kOe. The field-increasing



section of the $M(H)$ curve can be fitted (**Supplementary Figure S2**) by a Langevin function:

$$M(H) = M_S \left(\coth(x) - \frac{1}{x} \right) \quad (1)$$

where $x \equiv \mu H/k_B T$, μ is the mean moment of the magnetic domains, k_B is the Boltzmann's constant, and M_S is the saturation magnetization. The Langevin function is understood to represent the alignment of magnetic moments by H , indicating that there are magnetic domains that can be polarized by H . This agrees with the ferromagnetic behavior suggested by the $M(T)$ curves. The saturation magnetization obtained from the fit is 25.6 emu/g at 5 K, corresponding to an average atomic moment of $0.3 \mu_B$. The magnetic hysteresis is clearly seen at 5 K, as shown in the inset in **Figure 3A**. The coercivity field obtained at 5 K is 29 Oe.

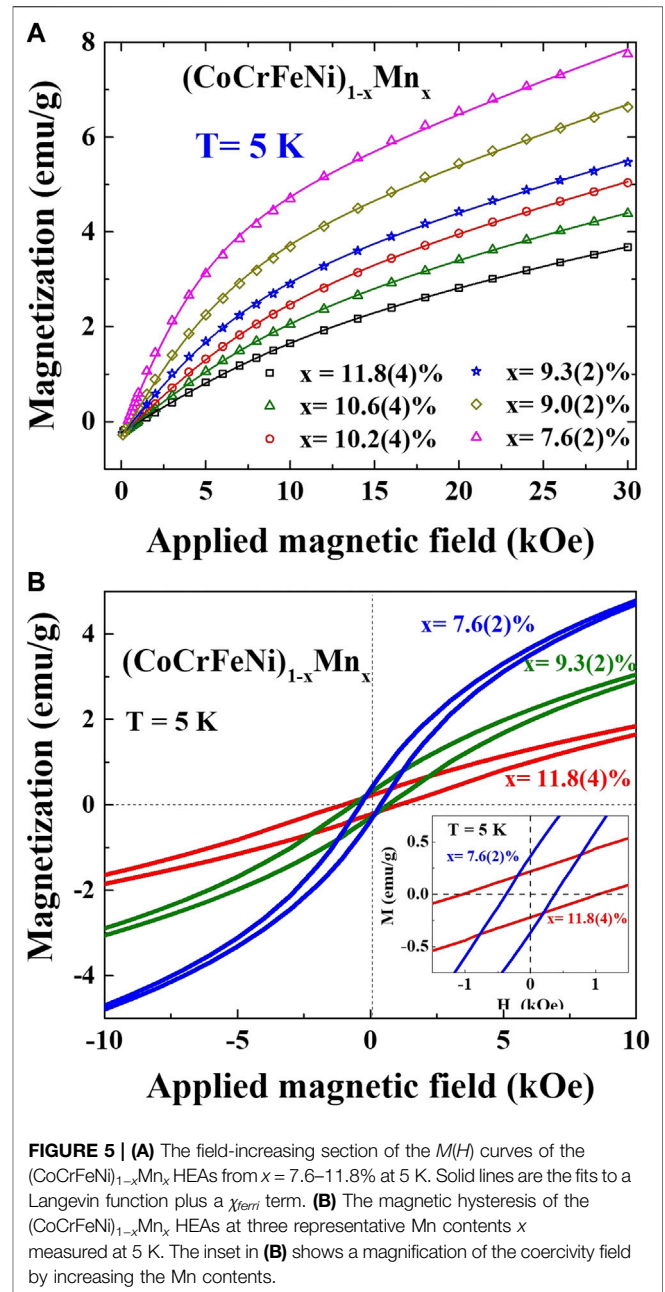


Figure 3B displays the $M(H)$ curves of the 7.6 (2)% Mn-incorporated $(\text{CoCrFeNi})_{1-x}\text{Mn}_x$ HEA taken at several temperatures. Interestingly, the field-increasing section of the $M(H)$ curve of the $(\text{CoCrFeNi})_{1-x}\text{Mn}_x$ HEA at $x = 7.6\%$ cannot be fitted only by a Langevin function (**Supplementary Figure S3**)—a positive linear term is also needed. The $M(H)$ curves can be described very well by a Langevin profile plus a positive linear term (**Supplementary Figure S3**):

$$M(H) = M_S \left(\coth(x) - \frac{1}{x} \right) + \chi_{ferri} H \quad (2)$$

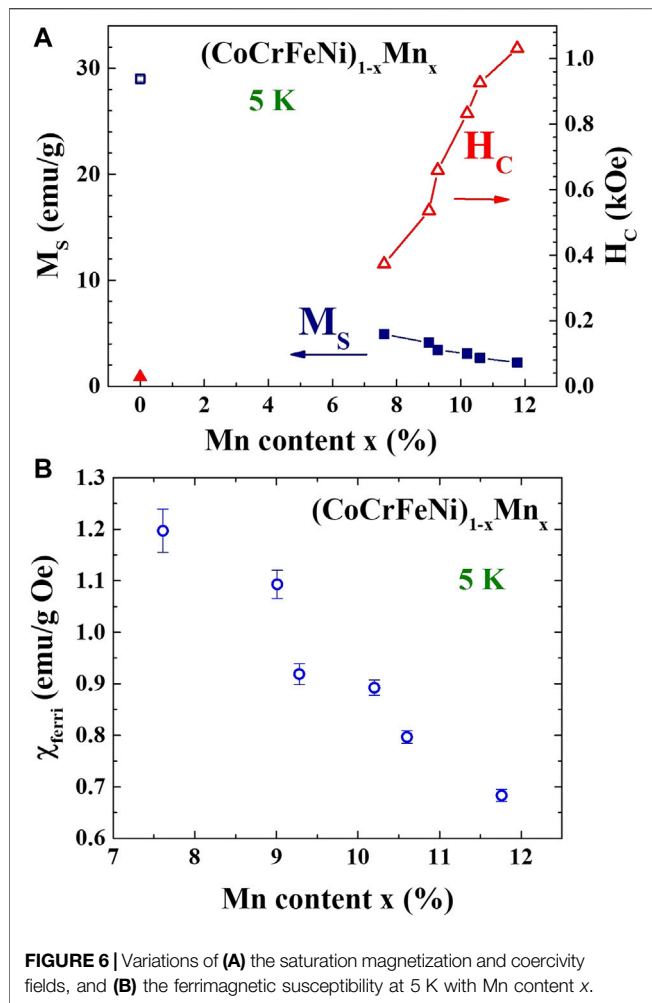


FIGURE 6 | Variations of (A) the saturation magnetization and coercivity fields, and (B) the ferrimagnetic susceptibility at 5 K with Mn content x .

where χ_{ferri} is the ferrimagnetic susceptibility, $x \equiv \mu H/k_B T$, μ is the mean moment of the magnetic domains, k_B is Boltzmann's constant, and M_S is the saturation magnetization. The positive linear term may be understood as the flip from the anti-parallel spins to the parallel direction by the applied magnetic field, whereas the Langevin profile reveals the polarization of the ferrimagnetic domains by the magnetic field. The magnetic properties in the $M(T)$ and $M(H)$ curves indicate a possible ferrimagnetic behavior in the Mn-incorporated (CoCrFeNi)_{1-x}Mn_x HEAs.

Figure 4A displays the $M(T)$ curves of the (CoCrFeNi)_{1-x}Mn_x HEAs with various Mn contents. The magnetization was suppressed significantly by the incorporation of the Mn atoms. All of the $M(T)$ curves follow the Curie-Weiss law (**Supplementary Figure S1**). The positive intercept of the $1/M$ trace with the temperature axis, together with a drop of the magnetization below ~ 15 K, indicates that the ferrimagnetism persists up to $x = 11.8\%$. The ferrimagnetic transition temperatures are determined by the dM/dT curves (inset of **Figure 4A**). The transition temperatures T_M can be enhanced by the Mn atoms (**Figure 4B**), indicating the energy of exchange

coupling between the Mn and Co, Cr, Fe, and Ni is higher than that between Co, Cr, Fe, and Ni.

The field-increasing section of the $M(H)$ curves of the (CoCrFeNi)_{1-x}Mn_x HEAs at various Mn contents are plotted in **Figure 5A**. All of the $M(H)$ curves can be described by a Langevin profile plus a positive linear term (**Figure 5A**). The positive linear term reveals the ferrimagnetic behavior of the (CoCrFeNi)_{1-x}Mn_x HEAs. The ferrimagnetic susceptibility χ_{ferri} is defined as the slope of the linear term. The variations of the coercivity, saturation magnetization, and ferrimagnetic susceptibility with Mn content, plotted in **Figure 6**, can be obtained from the fits. The susceptibility χ_{ferri} appears to be smaller at high Mn contents, revealing that it is difficult for the applied magnetic field to flip the anti-parallel spins. The magnetic hysteresis is clearly seen in all curves, as shown in **Figure 5B**. As seen in **Figure 6**, the coercivity increases with the increase of Mn content, while the saturation magnetization decreases. The coercivity fields can be increased by 2.76 times by raising the Mn content from 7.6 (2) to 11.8 (4)%.

The saturation magnetization of 4.9 emu/g at 5 K in the (CoCrFeNi)_{1-x}Mn_x HEA at $x = 7.6\%$ was unexpectedly small compared to the Mn-free CoCrFeNi. The saturation magnetization was suppressed by up to 81%. The calculated spin-only magnetic moment for a Mn atom is $5.92 \mu_B$, which is larger than that of the average value ($4.38 \mu_B$) among Co, Cr, Fe, and Ni. Calculating using the spin-only values and assuming that the magnetic moment of Mn is the only moment that points in the opposite direction, we expect a 17.9% reduction in the saturation magnetization with 7.6 (2)% of Mn incorporated. That is, 7.6 (2)% of the atoms with $4.38 \mu_B$ have been replaced by atoms with $-5.92 \mu_B$ from $x = 0$ –7.6%, giving a difference in moment of $-5.92 \mu_B \times 7.6\% - 4.38 \mu_B \times 7.6\% = 0.783 \mu_B$. This corresponds to a $0.783 \mu_B / 4.38 \mu_B = 17.9\%$ reduction. However, we observed an 81% reduction at $x = 7.6\%$, and the remaining 63.1% reduction cannot be explained solely by the inverse moment of Mn. Such a huge observed reduction (81%) indicates that the magnetic moments in some of the other elements (Co, Cr, Fe, and Ni) may have been flipped to the opposite direction by the exchange interaction with the Mn atoms. To contribute the remaining 63.1% reduction, $63.1\% / 2 = 32\%$ of the magnetic moments on the other elements need to be flipped. This indicates that 7.6 (2)% of Mn is enough to trigger the antiferromagnetic coupling between the other moments. For the FCC structure, there are twelve nearest neighbors surrounded by a Mn atom. On average, there are 4.3 atoms neighboring the Mn atom pointing in opposite directions. Theoretical and experimental results suggest that the antiferromagnetic couplings appear mostly on the Cr and Mn atoms in the equimolar CoCrFeMnNi HEA (Schneeweiss et al., 2017; Zuo et al., 2017). They also suggest that antiferromagnetic couplings may also appear on Ni, Fe, and Co atoms, but with a lower probability.

At the highest Mn content ($x = 11.8\%$) in the studied (CoCrFeNi)_{1-x}Mn_x HEA systems, we expect a $(5.92 \mu_B \times 11.8\% + 4.38 \mu_B \times 11.8\%) / 4.38 \mu_B = 27.4\%$ reduction of the saturation magnetization based on the spin-only values. However, we observed a 91% reduction of the saturation

magnetization at $x = 11.8\%$. The remaining $91 - 27.4\% = 63.6\%$ reduction may be attributed to the flipped magnetic moments of the other elements (Co, Cr, Fe, and Ni) due to the exchange interaction with the Mn atoms. To contribute the remaining 63.6% of reduction, $63.6\%/2 = 32\%$ of the magnetic moments on the other elements need to be flipped. In fact, 32% is also the value expected for (CoCrFeNi)_{92.4}Mn_{7.6}, which has low Mn content ($x = 7.6\%$). The reduction in magnetization from 81 to 91% is proportional to increasing the Mn content from 7.6 (2)% to 11.8 (4)%. The inverse relationship between magnetization reduction and increased Mn content is based on the mechanism that the increase of Mn will increase the number of spins that point in the opposite direction. Compared with 7.6 (2)% Mn, 11.8 (4)% Mn does not induce more antiparallel moments in Co, Cr, Fe, and Ni. This shows that 7.6 (2)% Mn is the upper limit of our system to saturate the antiferromagnetic couplings between the other atoms.

According to the Bethe–Slater curve (Slater, 1930a; Slater, 1930b), the sign of the exchange coupling integral J can be estimated from the ratio between the interatomic distance D and the diameter of the 3d orbital r . The negative J , giving the antiferromagnetic couplings, is estimated to appear at small D/r . On the other hand, at large D/r , J becomes very weak because of the long interatomic distance, resulting in the paramagnetic behavior. The ferromagnetic behavior, with positive J , appears at the intermediate D/r value between the antiferromagnetic and paramagnetic behaviors. In this work, the lattice constants for $x = 0, 7.6\%$, and 11.8% are 3.570, 3.583, and 3.588 Å, corresponding to the distances D of 2.520, 2.533, and 2.536 Å, respectively. The average diameters r are 1.528, 1.545, and 1.555 Å for $x = 0, 7.6\%$, and 11.8% , respectively. This gives a 1.0% reduction in the D/r ratio from $x = 0 - 11.8\%$. The incorporation of the Mn atoms leads to a relatively smaller D/r ratio, resulting in the greater possibility of antiparallel alignment of the magnetic moments.

On the other hand, magnetic frustration caused by the presence of the Cr atoms was expected in the body-centered cubic (BCC) Fe–Cr alloy according to density functional theory [DFT (Klaver et al., 2006)]. At a Cr content near 50%, the magnitudes of the antiferromagnetically aligned Cr moments were reduced to nearly zero by the frustration, giving it a ferromagnetic behavior. In the BCC Fe–Mn alloy, the flipping of the Mn moments by increasing Mn contents was also predicted by DFT calculations and spin Monte Carlo simulations (Schneider et al., 2021). Furthermore, the FCC lattice is the best-known frustrated antiferromagnet (Coey, 2010). The FCC (CoCrFeNi)_{1-x}Mn_x HEA may exhibit a more significant frustration than the BCC Fe–Cr alloy expected by Klaver et al. (2006). However, from the *ab initio* calculation, the appearance of the Mn atoms in the FCC CoCrFeNiMn HEA stabilizes the antiferromagnetic configurations (Wu et al., 2020). In our Mn-free equimolar CoCrFeNi HEA, the 25% Cr content exceeds the dilute limit of 8% of the magnetic frustration proposed by Klaver et al. (2006). A significant magnetic frustration took place, resulting in the possible ferromagnetism in the Mn-free CoCrFeNi HEA. When the presence of the Mn atoms

stabilizes the antiferromagnetic configuration, the system will become antiferromagnetic.

The exchange interactions in (CoCrFeNi)_{1-x}Mn_x HEAs are extremely complicated. The equimolar CoCrFeNiMn FCC random solid solution has been investigated *via ab initio* calculations (Schneeweiss et al., 2017). The combined special quasirandom structure (SQS) and Vienna Ab initio Simulation Package (VASP) results by Schneeweiss *et al.* suggest the ferromagnetic ordering of the Ni and Co moments. In contrast, the Fe, Cr, and Mn moments prefer to align antiferromagnetically. Our experimental results suggest that there are at least three elements aligned antiferromagnetically in the incorporation of the Mn atoms. The Mn atoms may reverse the Fe and Cr moments to minimize the total energy.

The saturation magnetizations of the (CoCrFeNi)_{1-x}Mn_x HEAs are smaller than those of ferrites, which are the best-known ferrimagnets. There are large amounts of antiferromagnetically aligned moments to cancel out the total magnetic moment. However, ferrites exhibit high electrical resistivity, which is suitable for high-frequency applications. The metallic (CoCrFeNi)_{1-x}Mn_x HEAs are electrically conductive, which is suitable for magnetic-damping or low-frequency applications.

CONCLUSION

In this report, we demonstrated the magnetic behavior of (CoCrFeNi)_{1-x}Mn_x high-entropy alloys (HEA). The Mn-free CoCrFeNi HEAs exhibited ferromagnetic behavior. However, a shift from ferro- to ferrimagnetism caused by the incorporation of Mn atoms into the CoCrFeNi HEA was identified. We observed an unexpected 81% reduction of the saturation magnetization with only 7.6 (2)% incorporation of Mn atoms. This indicates that the Mn triggered the neighboring moments to align in antiparallel directions. However, in our systems, this effect of increased Mn content has an upper bound of 11.8 (4)%, after which it does not increase the antiparallel moments of neighboring atoms as effectively as with smaller amounts of Mn. The ferrimagnetic transition temperature increased by 13% from $x = 7.6 - 11.8\%$, showing the exchange coupling strength from Mn atoms is slightly stronger.

DATA AVAILABILITY STATEMENT

The original contributions presented in the study are included in the article/**Supplementary Material**, further inquiries can be directed to the corresponding authors.

AUTHOR CONTRIBUTIONS

C-HL, C-CW, and E-WH designed the study; H-HC and K-YZ performed the measurements; C-HL and H-HC analyzed the data; Y-JC, A-CY, J-WY, S-JL, and UG fabricated the samples; all

of the authors discussed the results; C-HL and E-WH wrote the manuscript.

ACKNOWLEDGMENTS

We thank the Ministry of Science and Technology (MOST) Programs 108-2221-E-009-131-MY4, 110-2224-E-007-001, and 108-2218-E-007-056. The authors sincerely appreciate the support from the High Entropy Materials Center of the National Tsing Hua University from The Featured Areas Research Center Program within the framework of the Higher

Education Sprout Project by the Ministry of Education (MOE) in Taiwan. Use of the high-performance, low-temperature, and multi-function X-ray diffractometer belonging to the Core Facility Center of National Yang Ming Chiao Tung University is supported by the MOST Program.

SUPPLEMENTARY MATERIAL

The Supplementary Material for this article can be found online at: <https://www.frontiersin.org/articles/10.3389/fmats.2022.824285/full#supplementary-material>

REFERENCES

- Acet, M. (2019). Inducing strong Magnetism in Cr₂₀Mn₂₀Fe₂₀Co₂₀Ni₂₀ High-Entropy Alloys by Exploiting its Anti-invar Property. *AIP Adv.* 9, 095037. doi:10.1063/1.5120251
- Chaudhary, V., Banerjee, R., Gwalani, B., Ramanujan, R. V., and Soni, V. (2020). Influence of Non-magnetic Cu on Enhancing the Low Temperature Magnetic Properties and Curie Temperature of FeCoNiCrCu(x) High Entropy Alloys. *Scripta Materialia* 182, 99–103. doi:10.1016/j.scriptamat.2020.02.037
- Chaudhary, V., Chaudhary, R., Banerjee, R., and Ramanujan, R. (2021). Accelerated and Conventional Development of Magnetic High Entropy Alloys. *Mater. Today* 49, 231–252. doi:10.1016/j.mattod.2021.03.018
- Coe, J. M. (2010). *Magnetism and Magnetic Materials*. Cambridge University Press.
- Cong, D., Rule, K. C., Li, W.-H., Lee, C.-H., Zhang, Q., Wang, H., et al. (2016). Confined Martensitic Phase Transformation Kinetics and Lattice Dynamics in Ni-Co-Fe-Ga Shape Memory Alloys. *Acta Materialia* 110, 200–206. doi:10.1016/j.actamat.2016.03.008
- George, E. P., Raabe, D., and Ritchie, R. O. (2019). High-entropy Alloys. *Nat. Rev. Mater.* 4, 515–534. doi:10.1038/s41578-019-0121-4
- Gludovatz, B., Hohenwarter, A., Catoor, D., Chang, E. H., George, E. P., and Ritchie, R. O. (2014). A Fracture-Resistant High-Entropy alloy for Cryogenic Applications. *Science* 345, 1153–1158. doi:10.1126/science.1254581
- Hariharan, V. S., Karati, A., Parida, T., John, R., Babu, D. A., and Murty, B. S. (2020). Effect of Al Addition and Homogenization Treatment on the Magnetic Properties of CoFeMnNi High-Entropy alloy. *J. Mater. Sci.* 55, 17204–17217. doi:10.1007/s10853-020-05171-8
- Huang, E.-W., Hung, G.-Y., Lee, S. Y., Jain, J., Chang, K.-P., Chou, J. J., et al. (2020). Mechanical and Magnetic Properties of the High-Entropy Alloys for Combinatorial Approaches. *Crystals* 10, 200. doi:10.3390/cryst10030200
- Kao, Y.-F., Chen, S.-K., Chen, T.-J., Chu, P.-C., Yeh, J.-W., and Lin, S.-J. (2011). Electrical, Magnetic, and Hall Properties of Al_xCoCrFeNi High-Entropy Alloys. *J. Alloys Compd.* 509, 1607–1614. doi:10.1016/j.jallcom.2010.10.210
- Kittel, C., Mceuen, P., and Mceuen, P. (1996). *Introduction to Solid State Physics*. New York: Wiley.
- Klaver, T., Drautz, R., and Finnis, M. (2006). Magnetism and Thermodynamics of Defect-free Fe-Cr Alloys. *Phys. Rev. B* 74, 094435. doi:10.1103/physrevb.74.094435
- Koželj, P., Vrtnik, S., Jelen, A., Krnel, M., Gačnik, D., Dražič, G., et al. (2019). Discovery of a FeCoNiPdCu High-Entropy Alloy with Excellent Magnetic Softness. *Adv. Eng. Mater.* 21, 1801055. doi:10.1002/adem.201801055
- Lucas, M. S., Belyea, D., Bauer, C., Bryant, N., Michel, E., Turgut, Z., et al. (2013). Thermomagnetic Analysis of FeCoCrNi Alloys: Magnetic Entropy of High-Entropy Alloys. *J. Appl. Phys.* 113, 17A923. doi:10.1063/1.4798340
- Na, S.-M., Lambert, P. K., and Jones, N. J. (2021). Hard Magnetic Properties of FeCoNiAlCuXTiX Based High Entropy Alloys. *AIP Adv.* 11, 015210. doi:10.1063/9.0000097
- Otto, F., Dlouhý, A., Somsen, C., Bei, H., Eggeler, G., and George, E. P. (2013). The Influences of Temperature and Microstructure on the Tensile Properties of a Education Sprout Project by the Ministry of Education (MOE) in Taiwan. Use of the high-performance, low-temperature, and multi-function X-ray diffractometer belonging to the Core Facility Center of National Yang Ming Chiao Tung University is supported by the MOST Program.
- CoCrFeMnNi High-Entropy alloy. *Acta Materialia* 61, 5743–5755. doi:10.1016/j.actamat.2013.06.018
- Schneeweiss, O., Friák, M., Dudová, M., Holec, D., Šob, M., Kriegner, D., et al. (2017). Magnetic Properties of the CrMnFeCoNi High-Entropy alloy. *Phys. Rev. B* 96, 014437. doi:10.1103/physrevb.96.014437
- Schneider, A., Fu, C.-C., Waseda, O., Barreteau, C., and Hicel, T. (2021). Ab Initio based Models for Temperature-dependent Magnetochemical Interplay in Bcc Fe-Mn Alloys. *Phys. Rev. B* 103, 024421. doi:10.1103/physrevb.103.024421
- Slater, J. C. (1930a). Atomic Shielding Constants. *Phys. Rev.* 36, 57–64. doi:10.1103/physrev.36.57
- Slater, J. C. (1930b). Cohesion in Monovalent Metals. *Phys. Rev.* 35, 509–529. doi:10.1103/physrev.35.509
- Song, H., Tian, F., Hu, Q.-M., Vitos, L., Wang, Y., Shen, J., et al. (2017). Local Lattice Distortion in High-Entropy Alloys. *Phys. Rev. Mater.* 1, 023404. doi:10.1103/physrevmaterials.1.023404
- Wu, X., Li, Z., Rao, Z., Ikeda, Y., Dutta, B., Körmann, F., et al. (2020). Role of Magnetic Ordering for the Design of Quinary TWIP-TRIP High Entropy Alloys. *Phys. Rev. Mater.* 4, 033601. doi:10.1103/physrevmaterials.4.033601
- Ye, Y. F., Wang, Q., Lu, J., Liu, C. T., and Yang, Y. (2016). High-entropy alloy: Challenges and Prospects. *Mater. Today* 19, 349–362. doi:10.1016/j.mattod.2015.11.026
- Yeh, J.-W., Chen, S.-K., Lin, S.-J., Gan, J.-Y., Chin, T.-S., Shun, T.-T., et al. (2004). Nanostructured High-Entropy Alloys with Multiple Principal Elements: Novel Alloy Design Concepts and Outcomes. *Adv. Eng. Mater.* 6, 299–303. doi:10.1002/adem.200300567
- Zuo, T., Gao, M. C., Ouyang, L., Yang, X., Cheng, Y., Feng, R., et al. (2017). Tailoring Magnetic Behavior of CoFeMnNiX (X = Al, Cr, Ga, and Sn) High Entropy Alloys by Metal Doping. *Acta Materialia* 130, 10–18. doi:10.1016/j.actamat.2017.03.013

Conflict of Interest: The authors declare that the research was conducted in the absence of any commercial or financial relationships that could be construed as a potential conflict of interest.

Publisher's Note: All claims expressed in this article are solely those of the authors and do not necessarily represent those of their affiliated organizations, or those of the publisher, the editors and the reviewers. Any product that may be evaluated in this article, or claim that may be made by its manufacturer, is not guaranteed or endorsed by the publisher.

Copyright © 2022 Lee, Chin, Zeng, Chang, Yeh, Yeh, Lin, Wang, Glatzel and Huang. This is an open-access article distributed under the terms of the Creative Commons Attribution License (CC BY). The use, distribution or reproduction in other forums is permitted, provided the original author(s) and the copyright owner(s) are credited and that the original publication in this journal is cited, in accordance with accepted academic practice. No use, distribution or reproduction is permitted which does not comply with these terms.